Volume 1 | Number 1 | Jan 2013 | Pages 1–100

Journal of
Materials Chemistry B

Materials for biology and medicine
www.rsc.org/materialsB

ROYAL SOCIETY
OF CHEMISTRY

ROYAL SOCIETY
OF CHEMISTRY

www.rsc.org/materialsB

Nanoparticle based fluorescence resonance energy transfer (FRET) for biosensing applications

Jingyu Shi,[a] Feng Tian,[a] Jing Lyu[a] and Mo Yang*[a]

[a] *Interdisciplinary Division of Biomedical Engineering, the Hong Kong Polytechnic University, Hung Hom, Kowloon, Hong Kong, P.R. China. E-mail:Mo.Yang@polyu.edu.hk; Fax: 852 2334 2429; Tel: 852 2766 4946;*

In the past decades, Förster resonance energy transfer (FRET) has been used as a powerful tool to provide nanoscale information in many biosensing and bioanalysis applications. The performance of FRET assay is mainly dependent on the design of donor and acceptor pairs. Recently, a series of nanoparticles start to be used in FRET assays including semiconductor quantum dots (QDs), graphene quantum dots (GQDs), upconversion nanoparticles (UCNPs), gold nanoparticles (AuNPs) and graphene oxide (GO). The rapid pace of development in nanoparticles provides a lot of opportunities to revolutionize FRET techniques. Many nanoparticle based FRET assays have also been developed for various biosensing applications with higher sensitivity and better stability compared with traditional organic fluorophore based FRET assays. This article reviews the recent progress of nanoparticle FRET assays and their applications in biosensing area.

1. Introduction

In the past decades, Förster or fluorescence resonance energy transfer (FRET) has been widely applied as a valuable tool to measure accurate nano-scaled information in biomedical and clinical applications.[1-2] FRET is a non-radiative phenomenon with the energy transferred from an excited donor fluorophore to an acceptor fluorophore by means of intermolecular dipole-dipole coupling.[1] FRET can only occurs when the intermolecular distance between donor and acceptor is smaller than 10 nm, which makes FRET a very sensitive technology for detection of near-field interaction between molecules.[5] In this close proximity, an excited donor molecule emits a virtual photon which is then absorbed by an acceptor molecule. The virtual photon is the non-radiative energy from the excited donor which is not measurable. The ability to transduce a near-field phenomenon to a far-field signal helps FRET obtain super-resolution well below the theoretical limit of light microscopy. FRET assays based on organic dyes have the advantages of simple preparation low cost. There are a huge number of organic dyes available for diverse applications. However, there are some limitations for these dyes. The weak signals, poor photobleaching resistance, short fluorescence life time and low chemical stability are continuous challenges for organic dye based FRET assays. Moreover, the toxicity of organic dyes makes them not suitable for intracellular applications.[3] Fluorescence protein (FP) based FRET assays permit experiments in living cells, which are able to detect dynamic intracellular interactions. However, they suffer from spectra cross-talk due to broad excitation/emission spectra and large size [4]. Therefore, the development

of new probes for both donors and acceptors is of high importance to overcome these disadvantages.

With the development of advanced nanoscience and nanotechnology, multiple promising nanoparticles with novel optical properties have injected fresh energy to FRET, giving a rebirth to FRET in medical and biological applications. Nanoparticles are particles with size ranging from 1 to 100 nm, possessing unique optical and electronic properties that are different from bulk materials. Most nanoparticles are associated with quantum size effect, which can provide nanoparticles with tunable optoelectronic properties by controlling their size and shape. When the size is small enough, the triggered quantum effect will offer nanoparticles with strong and stable luminescence with high quantum yield. These fluorescence nanoparticles including semiconductor quantum dots (QDs), graphene quantum dots (GQDs), and upconversion nanoparticles (UCNPs) have received considerable attention as photo-stable fluorescence probes which can be good candidates as donors in FRET. Moreover, nanoparticles with relatively large size have unique electronic properties which are responsible for super quenching ability. For example, gold nanoparticles (AuNPs) and graphene oxide (GO) can be used as efficient fluorescence quenchers in FRET assay.

In addition, most nanoparticles are of high surface to volume ratio, which various biomolecules immobilizations on nanoparticles' surface at the same time, thus facilitating the establishment of "single-to-multiple" FRET donor-acceptor models. As a consequence, the replacement of organic fluorescent dyes by nanoparticles would

bring the typical FRET system with surprising effects, such as high energy transfer efficiency, long-range working distance, and tunable spectra to minimize the crosstalk between donors and acceptors. Therefore, nanoparticle based FRET system is very promising for many biological applications including nucleic acid analysis, immunological bioassays, cancer cells detection, and drug delivery.

The purpose of this review is to present the recent advances and development of nanoparticle based FRET biosensors for medical and biological applications. In Section 2, history and mechanism of traditional FRETs are presented. Organic fluorescent dyes and fluorescent proteins based FRET assays are briefly discussed. Section 3 presents different types of nanoparticles as FRET donors, such as semiconductor quantum dots, graphene quantum dots, and upconversion nanoparticles. The development of fluorescent nanoparticles based FRET biosensor for biomedical applications is also presented. Section 4 discuses nanoparticles as FRET acceptors such as gold nanoparticles and graphene oxide in various biosensing applications. Finally, challenges and future directions are discussed in the conclusion section.

2. Traditional FRET assays

2.1 History and mechanism of FRET

The discovery of FRET phenomenon could be traced back to the beginning of twentieth century. In a famous experiment in 1922, Cario and Franck initially demonstrated the energy transfer from mercury to thallium atomic vapour.[6-7] After Jean Perrin initially put forth theoretical explanation of this process and named it to be

4

molecular transfer of energy ("transfert d'activation") in 1927.[8] J. Perrin proposed the dipole interactions would be responsible for the transferred energy between molecule and its neighbour under intermolecular distance over 1000 Å. Afterwards, Perrin's son Francis developed a corresponding quantum mechanical theory based on Kallmann and London's results in 1932.[9-10] And he recognized the influence of spectral overlap between emission spectrum of donor and absorption spectrum of acceptor on energy transfer efficiency. Francis also estimated the intermolecular distance where the energy transfer might occur. However, the average distance was calculated to be 250 Å, which was much larger than that of experimental evidence.[11]

Based on the contributions of Jean and Francis, Theodor Förster developed a quantitative theory to describe the non-radiative energy transfer depending on overlap spectrum and intermolecular distance. Förster correctly treated the rate of energy transfer in terms of spectral overlap integral.[5] The simplified equation of FRET efficiency is illustrated as following: [12]

$$E = \frac{1}{1+\left(\frac{R}{R_0}\right)^6} \qquad (1)$$

Where R is the distance between donor and acceptor, and R_0 is the fluorescent distance of donor and acceptor when the transfer efficiency is 50%. The energy transfer efficiency (E) is inversely proportional to the sixth power of the distance between donor and acceptor. The rate of transfer is about to reach the maximum with the decreasing distance R (less than R_0). Moreover, by means of overlap integral, Förster showed that R_0 could be calculated to be 10 − 100 Å, which was consistent with previous experimental results. As a result, it is possible to infer molecular

distance between donor and acceptor by calculating R_0 and measuring E. As FRET is highly tied to the change of distance-dependent fluorescence signal, it can be used to monitor quantitative and dynamic molecular interactions *in vitro* [13-15] or *in vivo*, [16-17] thus making FRET becomes one of the most sensitive tools to access molecular scale information.

2.2 Organic fluorescence dyes and fluorescence protein

Traditional FRET dyes are organic dyes that can emit from UV to near-infrared region. There are many types of fluorescent dyes, such as cyanine family, FAM, and Texas Red. The advantages of organic fluorescent dyes include small size, high quantum yields, solubility and ease of bioconjugation, which make them important for dye-to-dye FRET systems. The application of FRET dyes has a great impact on nucleic acid analysis. The fluorescent labeled DNA probe and target combined with FRET strategy make it possible to observe the DNA interaction by monitoring fluorescence signal change.[18-20] However, high photobleaching rate and pH-sensitivity are the major drawbacks of traditional dyes.

With the discovery of green fluorescence protein (GFP) in beautiful jellyfish by Osamu Shimomura,[21] fluorescence protein (FP) firstly came into the picture in 1962. After that, Martin Chalfie found the value of GFP, which could be considered as a fluorescent tag to observe previously invisible biological phenomena.[22] At 1990, Tsien initially expressed stable GFP in other organism, and produced different color of FP, including blue, cyan, and yellow (BFP, CFP, YFP).[23] At 2008, the Nobel Prize in

chemistry was awarded to Osamu Shimomura, Martin Chalfie, and Roger Y. Tsien for the discovery and development of GFP.

The cloned FP possesses crystalline β-can structure with well controlled N- or C-terminal. The size of FP is 4.2 nm in length and 2.4 nm in diameter.[24] The optical properties of FPs include good photostability, high quantum yield, and broad excitation and emission spectra. Genetically labeled fluorescent protein made the intracellular FRET popular to observe protein-protein interaction in living cells. When FP is used as a fluorescence donor in FRET system, the properties of good photostability and high quantum yield could ensure high FRET signal for reliable and long-term detection.[25, 27] However, the broad excitation and emission spectra of FP might cause the spectral cross-talk, which could induce the noise of back ground signal. The large size of protein might also hamper the efficiency of FRET by occupying the efficient FRET distance [26].

3. Nanoparticle as donors in FRET assay

To improve FRET efficiency and sensitivity, many efforts have been spent to look for new alternatives for both donors and acceptors to replace traditional organic dyes. Many nanoparticles including semiconductor quantum dots (QDs), graphene quantum dots (GQDs), rare-earth doped upconversion nanoparticles (UCNPs) have been used as FRET donors, providing higher efficiency, better stability and performance for biosensing. Table 1 shows the characteristics of some nanoparticles as FRET donors.

Table 1 Characteristics of some nanoparticles as FRET donors.

FRET donors	QDs	GQDs	UCNPs
Size	1-20 nm (tunable)	<100 nm	10-150 nm
Dimension	0D	0D	0D
Surface to volume ratio	high	high	high
Excitation wavelength	UV radiation	UV radiation	NIR radiation
Color (PL)	tunable PL (blue to red) narrow emission band	tunable PL (blue to red)	tunable PL narrow emission band
Solubility	control by surface chemistry	high	high
Quantum yield	10%–80% (visible), 20%–70% (NIR)	2-23% (visible) Amino-GQD-PEG (46%)	<1%
Fluorescence lifetime	10–100 ns, typically multi-exponential decay	Nanosecond range	Microsecond-millisecond range
Photostability	good	high	high
FRET pairs	single-donor–multiple-acceptor configurations	single-donor–multiple-acceptor configurations	single-donor–multiple-acceptor configurations
Toxicity	high	low	low
Chemical stability	low	good	good

3.1 Quantum dots as FRET donor

Quantum dots are highly luminescent semiconductor nanocrystals, comprising

hundreds to thousands of atoms, in which excitons are restricted in all three

dimensions. The most common QDs include CdSe, CdTe, InP and InGaP which have been used as fluorescence labels in various biological applications. Compared with traditional organic fluorescent probes, QDs have many advantages as FRET donors in multiple biological applications such as narrow and tunable emission spectra, negligible photobleaching, as well as long fluorescence life time.[28-31]

The tunable size of QDs between 1 to 20 nm could generate a wide range of fluorescence emission peaks with Gaussian emission distribution.[32] Generally, the primary feature of QDs is their quantum confinement effect, determined by the small diameter of a semiconductor crystallite as compared to the bulk exciton Bohr radius. As the size of QDs decrease, the confining region decreases and the bandgap widens, resulting in shorter wavelength of light emission. Nirmal and Brus observed that the fluorescence emission peak of QDs could be continuously tuned over almost the entire visible region by controlling the size of QDs.[33] So it is feasible to achieve narrow and customized emission spectrum of QDs and to realize the maximum spectra overlap between FRET pairs, therefore enhancing the FRET efficiency. QDs can be excited with a short-wavelength light source, usually in the UV region which is far away from the excitation spectrum of acceptor and thus excitation crosstalk can be minimized.[34-35] In this case, the disturbing background signal is significantly avoided, which enhances the sensitivity of FRET sensing.

In addition, QDs have better photostability and longer fluorescence life time under continuous light excitation compared with organic fluorophores.[36] QDs were usually surrounded by a protective shell or different coatings, which have higher band

gap energy than the core material, giving rise to higher quantum yield. For instance, quantum yield of CdSe QD increased from 5% to 50% with one or two monolayers of ZnS capping.[37] QDs are mostly used as FRET donors in various biosensing applications, where their photoluminescence properties allow the optimization of spectra overlap by tuning the size and minimization the crosstalk between quantum dot and the acceptor molecules. Moreover, the large surface area of QDs offers an opportunity for molecular adsorption or surface modification. As a consequence, one single QD donor can absorb or graft multiple acceptors simultaneously, which also increases the FRET efficiency. In some cases, QDs can also be used as acceptors due to the spectra overlap with some donor molecules such as UCNPs [38] and naphthalimide chromophore 1.[39]

For DNA detection, Zhang et al. designed a FRET based sandwich system using streptavidin coated CdSe-ZnS QD as a donor and organic fluorescence dyes Cy5 as an acceptor for target DNA detection.[40] Biotin was firstly conjugated with capture probes, while Cy5 was immobilized with the reporter probes (Fig.1). The sandwich structure was formed via the co-hybridization of target DNA with capture probes and reporter probes. Then, the strong affinity interaction between biotin and streptavidin would bring the Cy5 labeled sandwich hybrids and QDs into close proximity, leading to the FRET effect. By monitoring the fluorescence signal, this QD based FRET biosensor showed extraordinary performance with limit of detection (LOD) of 4.8 fM. Algar et al. developed a series of optical fiber based QD-FRET platforms for nucleic acid detection.[41-43] In this QD-FRET platform, QDs were firstly conjugated on

optical fibers with capture probes. Based on biotin-neutravidin conjugation, target

molecules with dye acceptors induced FRET effect for nucleic acid detection. The

LOD of this QD FRET sensor for DNA detection is from 1 nM to 10 nM. Kim et al.

developed a CdSe-ZnS QD conjugated molecular beacon, in which the luminescence

of QD was quenched by organic fluorescence dye DABCYL.[44] After hybridization

with addition of target DNA, the opening of the molecular beacon separated QD and

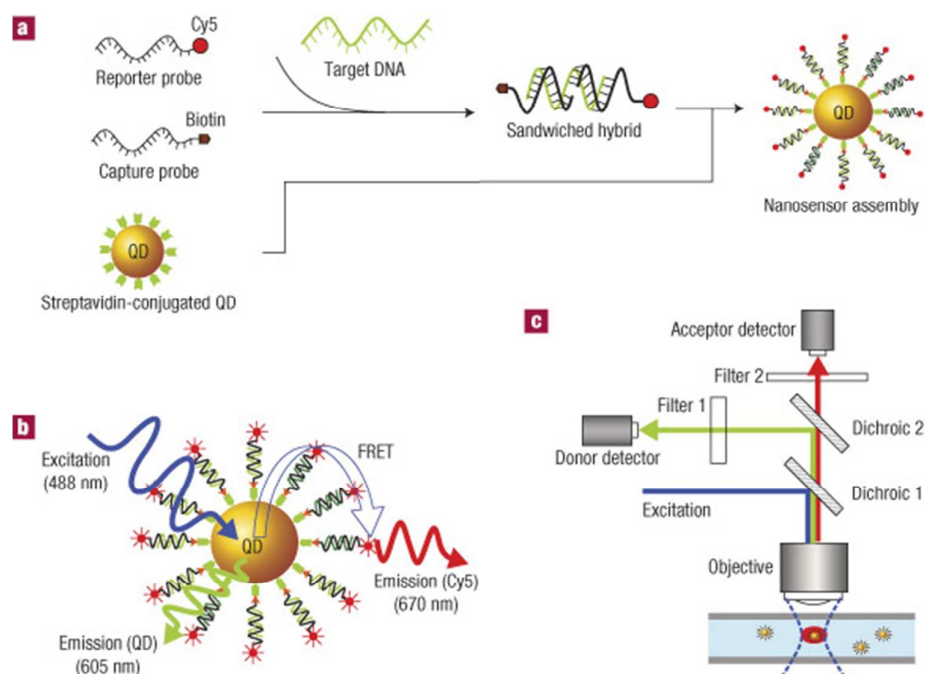DABCYL, resulting in the restored luminescence of QDs.

Fig. 1 Schematic diagram of single quantum dot based FRET nano-biosensor. Reprinted with permission from Ref. 40.

QD based FRET immunoassays have been used in many biomedical applications.

For protein analysis, antibodies or aptamers can be firstly conjugated on QDs to

generate QD-antibody or QD-aptamer FRET assays. The target proteins can then be

conjugated to QDs to trigger FRET process for protein detection. Wei et al. developed

a sandwich FRET immunoassay for estrogen receptor β concentration measurement

based on FRET between QD-labeled antibody and organic acceptor labeled polyclonal antibodies against estrogen receptor β.[45] Aptamers have also been used to conjugate QD to generate QD-aptamer FRET assay for the detection of thrombin and epithelial tumor marker.[46-47] QD-protein assays have also been used to detect the enzymatic activity of proteases [48] and kinases,[49] as well as to detect intracellular pH change.[50]

QD based FRET immunoassays are widely used for human disease diagnostics. One of the important applications is for cancer biomarker detection. Liu et al. developed a CdTe QDs-based FRET biosensor for the detection of the cancer marker type IV collagenase.[51] In the presence of type IV collagenase, the linking peptide between the donor molecule QD and the acceptor AuNP was cleaved which led to the recovery of fluorescence signals. The detection concentration range is 0.05–10 μg/mL with a LOD of 18 ng/mL. Cheng et al. developed a QD-aptamer FRET assay for epithelial tumor marker Mucin 1 (MUC1) detection.[52] In the presence of MUC1 peptides, the decrease of fluorescence signal was observed since peptides conjugated with aptamer to bring QDs and quenchers into close proximity. The LOD of this QD-aptamer FRET assay for MUC1 detection was in nM level. QD based assays have also been used for the sensing of caspase 3 activity, which is part of the apoptosis signaling pathway. Boeneman et al. developed a CdSe-ZnS QD based FRET assay for caspase 3 activity detection.[53] Caspase 3 cleavage site was firstly expressed in the red fluorescence protein mCherry and QD was then linked with mCherry to form the FRET assay. In the presence of caspase 3, the linking peptide was cleaved which

caused an increase of QD emission. The caspase 3 activity was monitored by observing the change of FRET efficiency. A detection limit of 20 pmol/L of caspase 3 was achieved. QD based FRET immunoassays have also been used for biomarker detection of other diseases including beta secretase inhibitor screening for Alzheimer's disease[54] and anti–topoisomerase I antibodies for systemic sclerosis autoimmune disease.[55]

A summary that lists the applications of QD FRET assays and their sensing parameters is provided in Table 2.

Table 2 Summary of QD FRET assays and their sensing parameters

Biological targets	Donor/Acceptor	Detection range	Limit of detection	References
DNA hybridization	QD/Cy5	4.8 fM to 96 nM	4.8 fM	Ref. [40]
DNA hybridization	QD/Cy3 on optical fiber	1 nM to 200 nM	1 nM to 10 nM	Ref. [41-43]
Estrogen receptor b (ER-b) antigen	QD/Alexa Fluor	0.05 nM to 50 nM	0.05 nM	Ref. [45]
Thrombin	QD/aptamer-dye	1 nM to 1 μM	1 nM	Ref. [46]
Cancer marker type IV collagenase	QD/AuNP	0.05–10 μg/mL	18 ng/mL	Ref. [51]
Cancer marker MUC1	QD/Iowa Black FQ quencher	250 nM- 2 μM	250 nM	Ref. [52]
Caspase-3 activity	QD/mCherry	N/A	20 pM	Ref. [53]
Beta secretase inhibitor	QD/AuNP	0.15 μM to 2.4 μM	0.15 μM	Ref. [54]

However, despite all the observable advantages, the limitations of QDs based

FRET strategy cannot be ignored. As FRET efficiency is susceptible to the distance between donor-acceptor pair, it is necessary to take the diameter of QDs and surface coating into consideration. The size of QDs ranges from 1 to 20 nm, which is typically larger than atoms, roughly equal to proteins, but smaller than bacteria.[32] Inevitably, the large size of QDs would impair the energy transfer efficiency of QD based FRET assays, making them less efficient than those with organic dyes.[56-57] Moreover, the synthesis procedures of conventional semiconductor QDs, such as CdSe, CdTe and CdSe-Zns, are always involved in toxic components, which hamper their development in the biological fields.[58-59]

3.2 Graphene quantum dots as FRET donors

Graphene has been regarded as theoretically existed material until Nobel laureates Geim and Novoselov successfully fabricated it in 2004.[60] Since then, researches associated with graphene have bloomed due to its unique thermal, mechanical and electronic properties.[61] Graphene is a 2D planar sheet of carbon atoms bonded in sp^2 hybridization with honeycomb-shaped lattice. However, as a zero band-gap semiconductor with the infinite exciton Bohr diameter, the luminescence of graphene is nearly impossible to be observed. [62] Thereby, graphene quantum dots (GQDs), the 0D graphene nanosheets, have emerged as extremely promising optoelectronic materials. Typically, GQDs are well-confined graphene nanosheets with diameter under 20 nm, which are small enough to trigger pronounced quantum confinement effect and edge effect. GQDs preserve several attributes of quantum dots,

14

such as tunable optical properties, high brightness, good photostability, and long fluorescence life time, making them to be excellent candidates for as FRET donors. Moreover, the excellent biocompatibility property makes GQDs FRET platforms quite suitable for biomedical applications.

The fabrication methods of GQDs can be classified in two routes: top-down methods [63-64, 68, 73-74] and bottom-up methods.[75-78] Considerable researches have demonstrated that GQDs synthesized by different methods possess varied size, physical and optical properties.[63-64, 68, 73-74, 75-78] For example, GQDs prepared by hydrothermal cutting had the size of 5 to 13 nm, containing less oxygen groups and emit blue luminescence,[63] whereas solvothermally and electrochemically synthesized GQDs with diameter of 3-5 nm could emit green fluorescence due to the abundant oxygen groups on the particle surface.[64,74] GQDs prepared by amino-hydrothermal approach (2.5 nm) or stepwise solution chemistry (2.5-5 nm) could emit yellow[68] or red [75] light, respectively. This phenomenon indicates that the PL of GQDs is a complicated phenomenon, which is dependent on several factors including the size of nanocrystal,[67] surface modification,[68-69] excitation wavelength,[70] pH environment,[63,71] and solvent types.[73] Unfortunately, since the discovery of GQDs is still in the initial phase, the universal PL mechanism of GQDs is still unclear. Generally, the tunable PL emission of GQDs can be achieved by manipulating the competition between intrinsic state emission and defect state emission,[72] which depends on the degree of surface defect in GQDs. Although the PL mechanism remains to be a mystery, strong and stable luminescence of GQDs is a striking

phenomenon, which ensures their application as fluorescence donors in long-term detection. Zhu et al. observed stable brightness of GQDs under continuous excitation for more than 20 min, which highlighted the negligible photobleaching and long fluorescence life-time of GQDs.[72] Furthermore, the quantum yield of GQDs ranges from 2% to 22% via various fabrication methods and it can be tuned by further surface fictionalization. According to Tetsuka et al., amine functionalized GQDs could emit green light with high quantum yield around 29~19%.[68] As GQDs is converted from graphene sheet, the property of high surface to volume ratio still remains. It offers large sensing area for molecular adsorption via π-π stacking interaction so that multiple fluorescence acceptors can attach to its surface that enhances the FRET efficiency significantly.[78] Nevertheless, when compared to conventional quantum dots (CdSe and CdSe-Zns), the most characterized advantages of GQDs are their non-toxicity and excellent biocompatibility, which promote the applications of GQDs in medicine and biology. According to Zhu et al. and Hu at al., MTT assay indicated that cells remained alive in the presence of high amount of GQDs,[66, 72] thus GQDs are more suitable for biological applications. Moreover, as carbon based luminescent nanomaterials, GQDs possess the advantages of easy fabrication and low cost compared to organic fluorescent dyes and fluorescent proteins.

Suprisingly, GQDs are shown to have upconversion PL properties. Shen et al. synthesied the PEG passivated GQDs, which showed upconverted emission at 525 nm when excited at 980 nm.[70] Besides, this upconversion luminescence also exhibited wavelength-dependent emission. When this PEG-GQDs were excited with excitation

wavelength ranging from 600 nm to 800 nm, the peak of upconverted emission showed red-shift from 390 nm to 468 nm, respectively. Similar results were also reported by Zhu et al. and Zhuo et al.[72-73] The upconversion luminescence of GQDs opens a door for near-IR light diagnosis using multi-photon excitation, which is less harmful to living biosystems compared to UV light.

However, in order to obtain real applications for GQDs, there remain some issues to be solved. For instance, excitation dependent effect of PL is still a problem that remains to be eliminated. Moreover, it is hard to accurately control the dimension and surface chemistry of GQDs. Most of the current studies are focused on facile fabrication methods for GQDs. In recent years, the further biomedical applications using GQDs just get started, such as bioimaging,[66, 71, 74, 79] biolabeling [65,80] and drug/gene delivery. [79, 81]

Most recently, GQDs started to be used as donors in FRET assays for biological applications. The emission spectra of GQD can be tuned by changing the size and surface modification which allows the optimization of spectra overlap with acceptor molecules. The fluorophore should be chosen for the spectra overlap between the emission spectra of the GQDs and the excitation spectra of the fluorophore. For DNA analysis, Shi et al developed a FRET biosensor with GQD as the donor and AuNP as the acceptor for food-borne pathogen *staphylococcus aureus* specific gene sequence detection.[82] This FRET biosensor platform was realized by immobilization of capture probes on GQDs and conjugation of reporter probes on AuNPs (Fig. 2). The oligo conjugated GQDs were observed to exhibit stronger luminescence with enhanced

quantum yield of 19% which was twice higher than that of bare GQDs. This could be explained by the decrease of oxidation degree induced by surface modification. The oxygen groups played a significant role in radiative recombination of localized electron-hole pairs and surface emissive traps of GQDs. The decreasing oxidation degree could alter sp^2 clusters and surface defects of GQDs, thus improving the quantum yield. Target oligos then co-hybridized with capture probes on GQDs and reporter probes on AuNPs to form a sandwich structure which brought donor and acceptor pairs to close proximity to trigger FRET effect. The limit of detection (LOD) of this GQD FRET biosensor was around 1 nM for *staphylococcus aureus* gene detection.
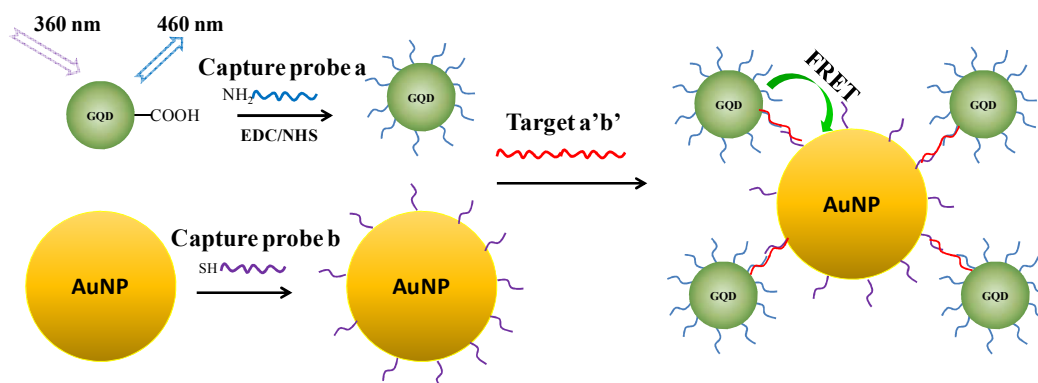

Fig.2 The sensing mechanism of the proposed GQDs–AuNPs FRET biosensor for S. aureus gene detection. Reprinted with permission from Ref. 82.

Qian et al developed a FRET assay with GQDs as donors and oxidized carbon nanotubes as acceptors for DNA detection. The FRET process was easily realized through specific π-π stacking between GQDs and carbon nanotubes. The detection limit of 0.4 nM was achieved by this FRET nanosensor.[83] Qian et al also developed a GQD FRET sensor with GO as acceptor for DNA detection.[84] In this sensor, complimentary DNA was firstly connected to GQD surface to achieve ssDNA-GQD

probe via a condensation reaction. Then ssDNA-GQD probe was immobilized on GO surface via π- π stacking to establish GQD-GO FRET assay. Upon the addition of target DNA, the hybridized double stranded DNA with GQD detached from GO surface. By measuring the recovery of fluorescence signal, DNA hybridization could be detected. The detection limit of this GQD-GO FRET assay was 75 pM for DNA detection.

GQD based FRET assay was also used as immunoassay for protein detection. Zhao et al. reported a FRET sensing strategy between GQDs and grapheme for sensitive detection of human immunoglobulin (IgG).[85] GQDs conjugated with anti-human immunoglobulin G (mIgG) were used as energy donors, and graphene sheets were served as energy acceptors (Fig. 3). Both the π-π stacking interaction between graphene and GQD and the non-specific binding interaction between graphene and mIgG would shorten the distance between GQD and graphene, leading to the fluorescence quenching effect. For human IgG detection, the specific antibody-antigen binding would increase the distance between GQD and graphene, restoring the fluorescence signal. By monitoring the fluorescence signal change, IgG could be detected in a linear concentration range from 0.2 μg/mL to 12 μg/mL. The detection limit was achieved with 10 ng/mL. Fan et al developed a GQD FRET assay for ultrasensitive detection of 2,4,6-trinitrotoluene (TNT).[86] TNT could specifically bind with fluorescent GQDs via π-π stacking interaction between GQDs and aromatic rings. This FRET assay could detect 0.495 ppm (2.2 μM) TNT with only 1 mL GQDs solution.

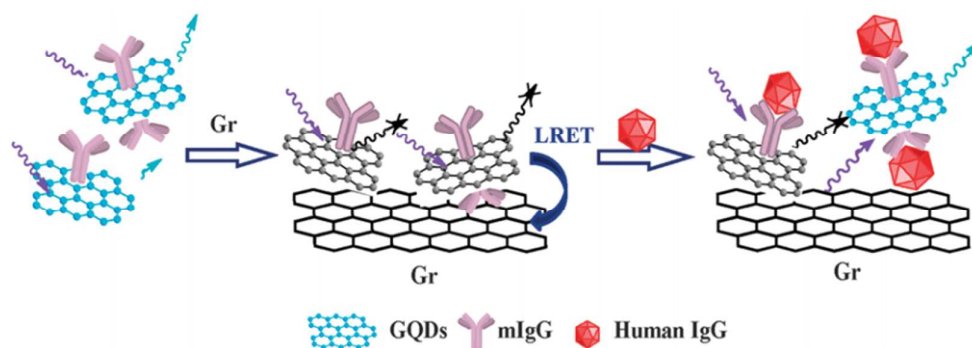A summary that lists the applications of GQD FRET assays and their sensing parameters is provided in Table 3.

Fig. 3 Schematic illustration of an immunosensor based on regulation of the interaction between Graphene and GQDs for human immunoglobulin detection. Reprinted with permission from Ref. 85.

Table 3 Summary of GQD FRET assays and their sensing parameters

Biological targets	Donor/Acceptor	Detection range	Limit of detection	References
Bacteria DNA	GQD/AuNP	1 nM to 100 nM	1 nM	Ref. [82]
DNA hybridization	GQD/CNT	0.4 nM to 133 nM	0.4 nM	Ref. [83]
DNA hybridization	GQD/GO	6.7 nM to 46.0 nM	75 pM	Ref. [84]
IgG	GQD/graphene	0.2 µg/mL to 12 µg/mL	10 ng/mL	Ref. [85]
TNT	GQD/TNT	0.495ppM to 181.58ppm	0.495ppM	Ref. [86]

3.3 Rare-Earth-Doped Upconversion nanoparticles (UCNPs) as FRET donors

Lanthanide-doped upconversion nanoparticles (UCNPs) as a new generation of fluorophores have aroused considerable attention in biological fields. They have big

potentials to be used as fluorescent labels because of their unique advantages as compared to organic fluorophores and QDs. For example, UCNPs have high quantum yield, narrow emission peak, large stoke shifts, good chemical stability and low toxicity.[87] These prominent merits make UCNPs to be promising candidates as donors applied in FRET-based biological detections. In addition, unlike QDs that need UV radiation, UCNPs can convert near infrared (NIR) (long-wavelength) radiation into visible light (short-wavelength fluorescence) via nonlinear optical processes.[88] It is widely known that NIR light with strong penetration ability is less harmful to biological samples. In contrast, UV light may cause photo damage to tissues. Thereby, UCNPs have been regarded as excellent alternatives to traditional fluorophores.

Lanthanide-based UCNPs are generally comprised of an inorganic host and lanthanide dopant ions as activator and sensitizer. Among various upconversion hosts, fluorides including $BaYF_5$, $NaYF_4$, KYF_4 and $NaLuF_4$ have been used because they can covert low phonon energy into visible light.[89-92] Dopant ions including Er^{3+}, Tm^{3+}, and Ho^{3+} are frequently used as activators to generate upconversion emission.[93-95] Yb^{3+} ion is the most popular sensitizer to achieve upconversion emission.[93-95]

UCNPs are generally used as donors in FRET assays which typically rely on coupling with a downconverting acceptor molecule. The fluorophore should be chosen for the spectra overlap between the emission spectra of the UCNPs and the excitation spectra of the downconverting fluorophores. Under NIR excitation, UCNPs' emission is in the visible light range which is necessary for excitation for

conventional fluorophores. The NIR excitation range makes UCNPs good donor candidates since NIR excitation light is far away from the excitation spectra of most acceptor molecules.

UCNP-organic dye based FRET assays have been developed for various biological applications.[96] Zhang et al. designed a sandwich-type energy transfer biosensor based on $NaYF_4$:Yb,Er UCNPs and fluorophore (TAMRA) for specific oligonucleotide sequence detection.[97] UCNPs and fluorophore were conjugated on the reporter and capture probes, respectively. The co-hybridization among target DNA, UCNPs-oligo and fluorophore-oligo would bring UCNP close to fluorophore, leading to the emission of fluorophore. By monitoring the emission of fluorophore, the target DNA could be detected sensitively and specifically with the detection limit of 1.3 nM. Similar sandwich-type nucleic acid biosensor based on $NaYF_4$:Yb Er UCNPs and fluorophore (TAMRA) was developed by Chen et al..[98] Hwang et al. developed UCNP- intercalating dye based FRET sensor for detecting the IS6110 sequence of the pathogenic bacteria *Mycobacterium tuberculosis* in sputum. *IS6110* DNA PCR amplicon was firstly mixed with streptavidin-conjugated UCNPs. By intercalation with SYTOX orange dye, fluorescence energy transfer was triggered between UCNPs and intercalating dye. The lowest detected concentration was 10^2 copies/μL.[99] Tu et al. developed a time-resolved FRET (TR-FRET) biosensor based on biotinylated $NaYF_4$:Ce/Tb UCNP and FITC labeled avidin for the detection of avidin.[100] The tight binding between avidin and biotin would bring UCNPs (donor) close enough to FITC (acceptor), leading to energy transfer. The detection limit of avidin was 4.8 nM.

In the same manner, Ju et al. developed a time-resolved FRET (TR-FRET) biosensor based on amino-functionalized $KGdF_4:Ln^{3+}$ UCNP and FITC labeled avidin for the detection of avidin. The detection limit of avidin was 5.5 nM.[101]

Recently, UCNP-graphene oxide (GO) FRET assays were developed for biosensing. Zhang et al. developed a LRET system based on UCNPs and GO for sensitive detection of glucose.[104] Concanavalin A (ConA) connected UCNPs were used as energy donors, and chitosan (CS) linked GO was functioned as energy acceptor. LRET occurred when UCNPs were close enough to GO duo to the specific binding between ConA and CS. However, the existence of glucose would abort FRET process because of the recognition between ConA and glucose, leading to the detachment of conA-UCNP from GO surface and hence restoring the luminescence. The plot of fluorescence intensity showed a linear relationship as a function of glucose concentration ranging from 0.56 to 2.0 µM. The detection limit of glucose was 0.025 µM. Alonso-Cristobal et al. developed a DNA biosensor based on fluorescence resonance energy transfer between NaYF4:Yb,Er nanoparticles and GO.[105] DNA functionalized UCNPs conjugated to GO surface via $\pi-\pi$ stacking which induced FRET based quenching. In the presence of complementary DNA, the hybridization led the double-stranded DNA detach from GO surface, and thus the recovery of fluorescent signal of UCNPs was observed. A detection limit of 5 pM was achieved for this UCNP-GO FRET assay.

UCNP-GO FRET immunoassays are also used for small biomolecules detection. Wu et al. presented a UCNPs-GO based LRET immunoassay for rapid and sensitive

detection of different mycotoxins, including ochrathoxin A (OTA) and fumonisin B_1 (FB_1).[102] $BaY_{0.78}F_5:Yb_{0.2}Er_{0.02}$ UCNPs conjugated with specific mycotoxin aptamers were used as donors. GO acted as a universal acceptor which could completely quench the luminescence of aptamer-UCNPs due to the close intermolecular distance caused by π-π stacking interaction. In contrast, in the presence of mycotoxins, the high affinity binding of aptamer-mycotoxin would excel the π-π coupling of GO-aptamer, resulting in negligible luminescence quenching. By monitoring the signal change, linear relationship between fluorescence intensity and concentration of mycotoxins can be obtained. The detection limits of OTA and FB_1 was 0.02 ng/mL and 0.1 ng/mL, respectively. Liu et al. demonstrated a LRET biosensing platform using β-$NaYF_4$:Yb,Er nanoparticles as the donor and GO as the acceptor for sensitive detection of adenosine triphosphate (ATP).[103] This UCNPs-GO based FRET biosensor showed a linear working curve with increasing ATP concentrations, ranging from 0.5 to 100 μM. The detection limit of ATP was 80 nM. Another carbon nanomaterial-carbon nanoparticles (CNPs) was also used as acceptor molecule in UCNP FRET biosensor for cancer biomarker matrix metalloproteinase-2 (MMP-2) detection.[106] Wang et al. used a polypeptide chain comprising MMP-2 substrate domain to link UCNPs and CNPs which initiated the FRET process.[106] Upon the cleavage of the linking peptide by MMP-2, the fluorescence signal was recovered which was proportional to the concentrations of MMP-2. The detection limit of this UCNP-CNP FRET assay for MMP-2 is as low as 10 pg/mL.

FRET assays based on UCNP-AuNP pair has also been developed for biosensing. Our group developed a biosensor based on BaGdF5:Yb/Er upconversion nanoparticles (UCNPs) and AuNPs for rapid and sensitive detection of short genes of H7 subtypes.[107] Generally, poly(ethylenimine) (PEI) modified BaGdF5:Yb/Er UCNPs was chemically conjugated with amino modified capture oligonucleotide probe. AuNPs was linked to thiol modified hemagglutinin H7 oligonucleotide sequence. The hybridization process between complementary strands of H7 Hemagglutinin gene and its probe brought the energy donor and acceptor into close proximity, leading to the quenching of fluorescence of UCNPs (Fig. 4). A linear response was obtained ranging from 10 pM to 10 nM and the limit of detection (LOD) is around 7 pM. This biosensor is expected to be a valuable diagnostic tool for rapid and sensitive detection of avian influenza virus (AIV). Wang et al. reported a LRET stragegy based on upconversion nanoparticles and AuNPs for avidin detecion.[108] Biotin-posphor nanoparticles was used as LRET donor, while biotin-Au nanoparticles was applied as LRET acceptors. In the presence of avidin, the specific binding between avidin and biotin would triger the fluorescence quenching of UCNPs by AuNPs. The linear working curve can be obtained as a function of the concentration of avidin ranging from 0.5 to 370 nM. Moreover, Wang et al. developed a sandwich structure assay based on LRET strategy for the detection of goat anti-human immunoglobulin G (IgG).[109] Rabbit antigoat IgG modified NaYF$_4$:Yb,Er UCNPs were used as energy donors, and human IgG conjugated AuNPs was employed as energy acceptors. A sandwich-type LRET system was generated with the presence of

goat anti-human IgG, which could bring UCNPs and AuNPs into close proximity through the specific immuno-recognition. By monitoring the fluorescence intensity, IgG could be sensitively detected in a linear concentration range from 3 to 67 µg/mL. The LOD of IgG was 0.88 µg/mL. Recently, Long et al. used UCNP-AuNP FRET biosensor for organophosphorus pesticides detection.[110] In the presence of acetylcholinesterase (AChE), acetylthiocholine (ATC) was hydrolyzed to generate thiocholine which resulted in the disintegration of the AuNPs/UCNPs assembly. With the addition of pesticide, the activity of acetylcholinesterase (AChE) was inhibited by pesticides, which could not stop the formation of AuNPs/UCNPs by electrostatic force. The formation of AuNPs/UCNPs complexes triggered the FRET effect. The detection limit of this UCNP-AuNP FRET assay for pesticide detection was in ng/mL level.

A summary that lists the applications of QD FRET assays and their sensing parameters is provided in Table 4.
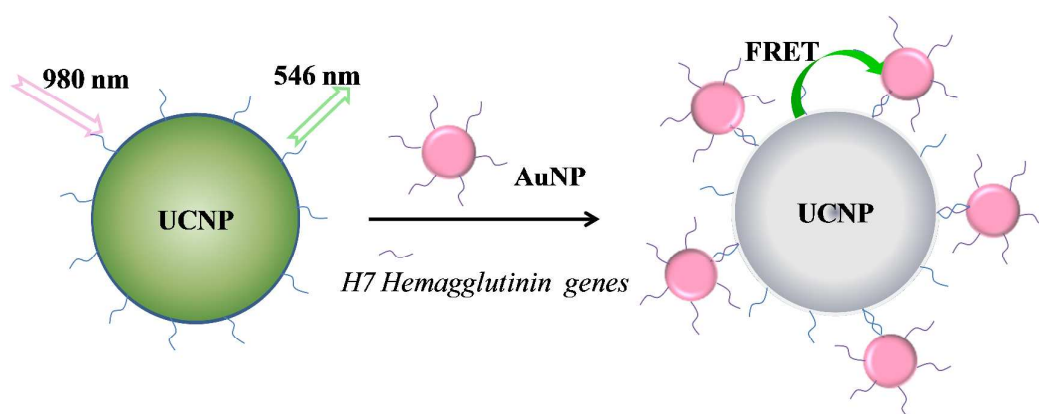

Fig.4 Sensing mechanism of H7 hemagglutinin gene detection by LRET biosensor based on energy transfer from $BaGdF_5$:Yb/Er UCNPs to AuNPs. Reprinted with permission from Ref. 107

Table 4 Summary of UCNP FRET assays and their sensing parameters

Biological targets	Donor/Acceptor	Detection range	Limit of detection	References
DNA hybridization	UCNP/TAMRA	1 nM to 60 nM	1.3 nM	Ref. [97]
Bacteria DNA	UCNP/SYTOX based PCR	N/A	10^2 copies/μL	Ref. [99]
Avidin	UCNP/FTIC	5 nM to 500 nM	4.8 nM	Ref. [100]
Avidin	UCNP/FTIC	4.5 nM to 1800 nM	5.5 nM	Ref. [101]
Glucose	UCNP/GO	0.56 to 2.0 μM.	0.025 μM	Ref. [104]
DNA hybridization	UCNP/GO	0.1 nM to 400 nM	5 pM	Ref. [105]
Mycotoxins OTA Mycotoxins FB1	UCNP/GO	0.05 to 100 ng/mL 0.1 to 500 ng·/mL	0.02 ng/mL 0.1 ng/mL	Ref. [102]
ATP	UCNP/GO	0.5 to 100 μM	80 nM	Ref. [103]
MMP-2	UCNP/CNP	10–500 pg/mL	10 pg/mL	Ref. [106]
Virus gene	UCNP/AuNP	10 pM to 10 nM	7 pM	Ref. [107]
Avidin	UCNP/AuNP	0.5 to 370 nM	0.5 nM	Ref. [108]
IgG	UCNP/AuNP	3 to 67 μg/mL.	0.88 μg/mL	Ref. [109]
Pesticides	UCNP/AuNP	0.2 ng/L to 20 μg/L	ng/L level	Ref. [110]

3.4 Solid-phase based nanoparticle FRET assay

Most of the current nanoparticle FRET diagnostic assays are solution-phase approaches which are time-consuming, labor intensive and not suitable for on-site screening. Moreover, the solution-based assays suffer from aggregation of nanoparticles and fluctuation of photoluminescence due to complex aqueous

environment. To overcome these drawbacks, solid-phase nanoparticle FRET assays have been used due to the advantages of simplicity, rapidity and possibility for high-throughput screening. Generally, in a solid-phase FRET assay, nanoparticle donors are firstly immobilized on a substrate and then interacted with functionalized acceptor molecules in the solution to trigger the FRET effect for detection.

Kim et al. designed a solid phase QDs based FRET multiplexed assay on a glass slide for matrix metalloproteinase-7 (MMP-7) protease activity detection.[111] For solid phase detection, QDs were firstly arrayed directly onto NHS-derivatized hydrogel glass slide in quadruple spot format by using a robotic arrayer. With the addition of peptide conjugated AuNPs, the fluorescence intensity of streptavidin-QD was quenched by biotinylated peptide labeled AuNPs through the formation of QD-peptide-AuNPs conjugates on the glass slide. Upon introduction of MMP-7 protease, the specific cleavage of peptide could cause the detachment of AuNPs from QDs, thus recovering the fluorescence signal. However, in the presence of MMP7 and their inhibitor, the change of fluorescence signal is negligible. By monitoring the signal change, the activity of MMP-7 was the logarithmic concentration of MMP-7 ranging from 10 ng/mL to 5μg/mL. Paper substrates have many advantages such as low cost, passive transport via capillary force, well established methods for surface modification and functionalization. Recently, Omair Noor et al. developed a paper-based solid-phase assay using QDs as donors for nucleic acid hybridization detection.[112] The detection limit of this assay was found to be 300 fmol without any amplification.

Fluorescent graphene nanoparticles have also been used in solid phase FRET assay. June et al. developed a fluorescent GO-AuNP FRET immuno-biosensor on a glass slide for pathogen detection.[113] Fluorescent GO was firstly synthesized and deposited on an amino-modified glass surface. Then the antibodies for rotavirus were immobilized on the GO array. When rotavirus cells were captured by the antibodies on GO surface, AuNP-linked antibodies were then added to form the sandwich structures. The close proximity between AuNPs and fluorescent GO surface caused FRET quenching. The detection limit of this GO-AuNP FRET assay was 10^5 pfu/mL for rotavirus detection. Shi et al. used a similar fluorescent GO-AuNP based FRET biosensor on a glass slide for bacterial toxin microcystin detection.[114] A positively charged glass slide by APTES silane modification was used as a substrate for GO array fabrication. Antibodies were then adsorbed on GO sheets via pi-pi stacking. When AuNP- microcystin complexes were captured by the antibodies on GO sheets, fluorescence signal of fluorescent GO was quenched as a result. The detection limit was 0.5 and 0.3 mg/L for microcystin-LR and microcystin-RR, respectively.

4. Nanoparticle as acceptors in FRET assay

This section will introduce gold nanoparticles (AuNPs) and graphene oxide (GO) as FRET acceptors, providing higher quenching efficiency and better performance for biosensing. Table 5 shows the characteristics comparison between AuNPs and GO as FRET acceptors.

Table 5 Characteristics of AuNPs and GO as FRET acceptors.

FRET acceptor	AuNPs	GO
Size	3-150 nm	Micro to nano scale (width)
		1 nm thickness
Structure	spherical	atomic flat layer
Dimension	0D	2D
Surface to volume ratio	high	high
Absorption spectra	450-550 nm	200- 800 nm
Quenching efficiency	$E\sim(R)^{-4}$	$E\sim(R)^{-4}$
Foerster distance (R_0)	70-100 nm	30 nm
FRET pairs	single-donor–multiple-acceptor	single-donor–multiple-acceptor
	configurations	configurations
Cost	relatively high	relatively low
Toxicity	relatively high	relatively low

4.1 GO as FRET acceptors

Graphene oxide (GO) is a derivative of graphene, usually synthesized by Hummer's method.[115] It possesses a similar 2D atomically layer to graphene, but equipped with carboxyl groups on the edges, hydroxyls and epoxies groups on the basal plane, which causes the co-existence of π state from sp^2 carbon clusters and σ state from sp^3 C-O matrix.[116] This unique heterogeneous electronic structure makes GO to be a super nano-quencher for universal fluorophores, including organic fluorescent dyes,[117-119] fluorescence proteins,[120] and quantum dots.[121-122] Therefore, GO has been widely used as an acceptor in FRET biosensing studies.

Generally, the wide absorption band of GO, ranging from 200 nm to 800 nm, allows FRET to occur without strict restriction of spectra overlap at a large degree.[127] As an excellent quencher, GO provides a longer-range working distance with higher FRET efficiency compared to typical FRET acceptor molecules. Large scale GO sheets are generally used as quenchers in FRET assays. With the size decreasing, nanoscale GO will gain photoluminescence properties such as GQD, which are often used as donors in FRET assays.

According to Swathi et al., the efficiency of resonance energy transfer between the fluorescent species and graphene was suggested to be higher with a $(distance)^{-4}$ dependence, as compared to $(distance)^{-6}$ dependent efficiency in traditional FRET.[123-124] And the effective working distance of this quenching effect was calculated to be as long as 30 nm, which was three times larger than that (10 nm) of conventional FRET. Similar super quenching ability of GO was also reported by Hung and Liu.[125] They made a use of varied DNA length to investigate distance dependent effect of GO in FRET, and the results were consistent with Swathi et al.'s calculation. Meanwhile, the thickness of GO is around 1 nm, while the width of GO ranges from micro to nano scale. This high surface to volume ratio also contributes to the super quenching efficiency due to the increasing contacting area that functions as FRET acceptors.[126] In another word, GO possess the capability of high loading amount of multiple fluorescent donors simultaneously, which is superior to traditional "one to one" FRET pairs. It is worth to mention that aromatic ring of GO can interact with the backbone of DNA or peptide via π-π stacking interactions,[128] which enables

31

a lot of possibilities in immobilization chemistry-free biosensors. Moreover, the super high fluorescence quenching efficiency of GO also brings the low background signals in detection, which improves the sensitivities of FRET sensing. The low cost of GO as carbon materials also gives promising opportunities to the development of GO based FRET sensing.

GO generally is used as an acceptor in FRET assays. Piao et al. demonstrated that GO usually serves as an acceptor rather than a donor in FRET system.[128] They fabricated a FRET donor, consisted of dsDNA with Cy3.5 dyes at one end and a polyA tail at another end. The π-π stacking between the polyA tail and GO would bring GO and Cy3.5 into close proximity, thus triggering FRET. Because GO could not absorb dsDNA, the distance-dependent FRET efficiency was investigated by controlling the length of dsDNA that functioned as spacer. The results demonstrated that the shorter spacer (5 or 7 bases DNA) exhibit higher quenching efficiency.

For DNA analysis, He et al. reported a homogeneous FRET sensing platform based on GO and multicolor fluorescent probes for specific DNA sequence detection.[129] The fluorescent dyes labeled probe DNA could be absorbed onto GO surface via π-π stacking interaction, resulting in the fluorescence quenching of dyes by GO. Upon addition of target DNA, the formation of dsDNA would release the dyes labeled probe DNA from GO surface, leading to the fluorescent signal recovery. The high quenching efficiency of GO ensured the minimal background signal so that this sensing platform exhibited high sensitivity in pM~nM range. In the same manner, Lu et al. fabricated a novel molecular beacon based sensor using GO as the FERT

quencher for specific target DNA detection.[130] The quenching efficiency of GO was as high as 99.1%, and the detection limit was around 2 nM.

GO can also immobilize with peptide via π-π coupling for corresponding protease detection. Shi et al developed a GO-peptide FRET assay to detect botulinum protein toxin enzymatic activity.[131] A green fluorescence protein (GFP) modified SNAP-25 peptide substrate (SNAP-25-GFP) was optimally designed and synthesized with the specific cleavage sites (Fig. 5). This FRET platform was constructed by covalent immobilization of peptide substrate onto GO surface followed by BSA passivation, which had advantages of low non-specific adsorption and high stability in protein abundant solution. As BoNT-LcA could specifically cleave SNAP-25-GFP substrate covalently immobilized on GO surface, GFP conjugated peptide fragment could be released into solution. Based on fluorescence signal recovery measurement, the target BoNT-LcA was detected sensitively and selectively with the linear detection range from 1 fg/mL to 1 pg/mL. The LOD for BoNT-LcA was around 1 fg/mL. When using GO as a quencher, the quenching efficiency of GO at certain concentrations could reach almost 100%, thus ensuring the low background signal and enhancing the sensitivity of this FRET biosensor at a large degree.
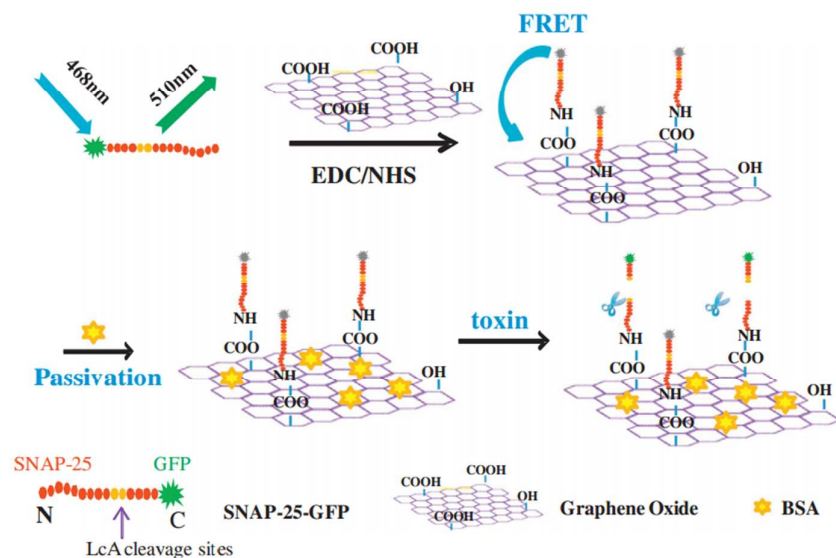
Fig.5 Sensing mechanism of GO based FRET biosensor for ultrasensitive detection of BoNT-LcA bacterial protein toxin enzymatic activity detection. Reprinted with permission from Ref. 131.

GO-peptide FRET based proteolytic cleavage assays have been used for various types of human biomarker detection. One important application is for cancer biomarker detection. Feng et al. designed a GO-peptide FRET sensing platform for real-time detection of matrix metalloproteinase 2 (MMP-2).[132] FITC labeled peptide with a specific cleavage site for MMP-2 was physically absorbed on GO surface, thus leading to fluorescence quenching of dyes. For MMP-2 detection, the specific cleavage of FITC-peptide by MMP-2 could cause the release of the peptide fragment with FITC into the solution, leading to the recovery of fluorescence signals. By monitoring the fluorescence signal, MMP-2 could be sensitively detected with a linear range from 0.2 to 2 nM with a detection limit of 50 pM. As MMP-2 is secreted by HeLa cells, thus the concentration of MMP-2 also revealed the density of HeLa cells.

Song et al. further improved this GO-peptide FRET system by immobilizing peptide on GO surface through covalent binding for MMP-2 detection.[133] Compared with the GO-peptide sensors with physical adsorption, this GO-peptide FRET sensor with covalent binding was more stable in physiological conditions. A rapid (within 3 hours) MMP-2 detection was achieved with a low detection limit of 2.5 ng/mL in complex biological samples.

GO based FRET immunoassays are also used for human biomarker detection. Wang et al. reported a simple and sensitive GO based FRET biosensor for the detection of cancer cell surface marker.[134] The sensing platform was initially at a quenching state due to the absorption of RGD-pyrene (donor) onto GO surface (acceptor) (Fig. 6). The quenching efficiency of GO was around 96%. However, the fluorescence intensity was gradually restored with the presence of integrin αvβ3 in the solution or overexpressed on the cancer cell membrane, because the high binding affinity between RGD-pyrene and integrin would release RGD-pyrene into the solution. Nearly 52% fluorescence signal of RGD-pyrene was recovered. Wang et al. developed a GO based aptamer sensor for detection of oncoprotein vascular endothelial growth factor (VEGF) in homogenous solutions.[135] The fluorescent dye-labeled anti-VEGF aptamer was firstly physically adsorbed on GO surface via pi-pi interaction, enabling the FRET effect. Upon binding with the target VEGF, VEGF/aptamer complex was formed and detached from GO surface, leading to the recovery of fluorescence signal. The detection limit of this GO based FRET sensor was around 0.25 nM.

QD-GO FRET assay was also applied for virus detection. Chen et al. designed a novel immunoassay based on dual-color QDs and GO for simultaneous detection of multiple viruses, including Human Enterovirus 71 (EV71) and Coxsackievirus B3 (CVB3).[136] Biotinylated EV71 antibody (Ab1) was firstly conjugated with streptavidin modified green QDs through biotin-streptavidin affinity interaction, forming QDs-Ab1 complex as fluorescence donors. Similarly, biotinylated CVB3 antibody (Ab2) was conjugated with red QD, forming QDs-Ab2 as fluorescence acceptors. The fluorescence of QDs-Ab1 and QDs-Ab2 was quenched by GO via π-π stacking interaction, generating a sensing platform for virus capture. In the presence of EV71 and CVB3, the specific binding between Abs and target viruses would break the absorption of QD-Abs to GO, restoring the fluorescence of QDs-Ab1 and QDs-Ab2. EV71 and CVB3 could be detected simultaneously with LOD of 0.42 and 0.39 ng/mL, respectively.

A summary that lists the applications of GO FRET assays and their sensing parameters is provided in Table 6.
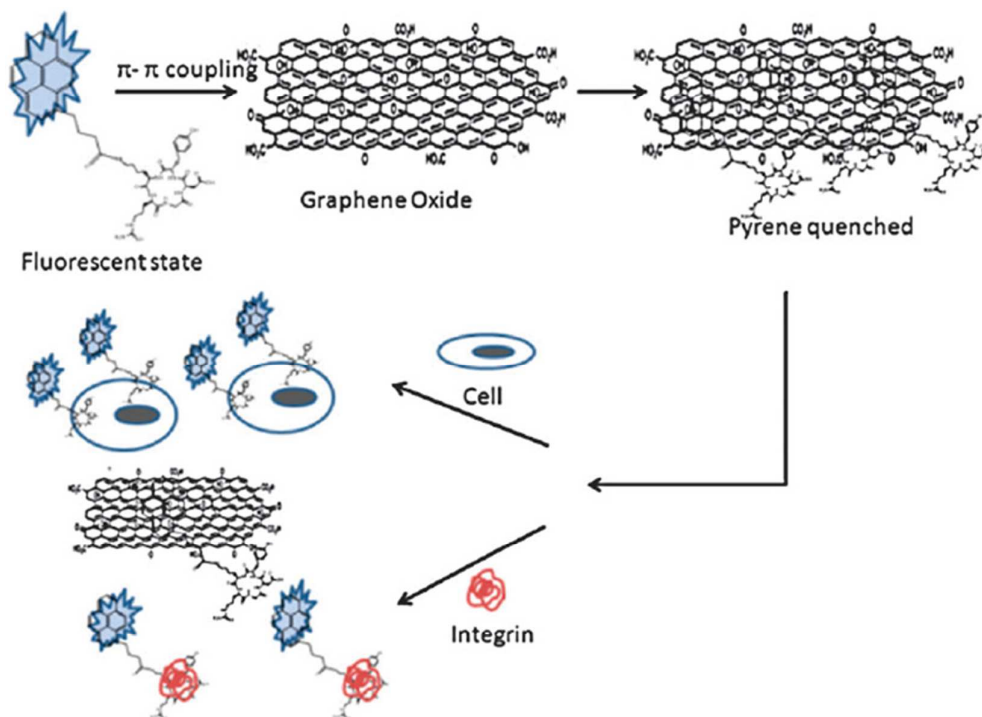
Fig. 6 Schematic illustration of a GO based FRET assay for detection of integrin αvβ3 protein or integrin over-expressing cancer cells. Reprinted with permission from Ref. 134.

Table 6 Summary of GO FRET assays and their sensing parameters

Biological targets	Donor/Acceptor	Detection range	Limit of detection	References
DNA hybridization	Fluorophore/GO	0 to 25 nM	100 pM	Ref. [129]
DNA hybridization	Fluorophore/GO	5 to 500 nm	2 nM	Ref. [130]
Bacteria toxin	Fluorophore/GO	1 fg/mL to 1 pg/mL	1 fg/mL	Ref. [131]
MMP-2	Fluorophore/GO	0.2 to 2 nM	50 pM	Ref. [132]
MMP-2	Fluorophore/GO	10 to 150 ng/mL	2.5 ng/mL	Ref. [133]
VEGF	Fluorophore/GO	N/A	0.25 nM	Ref. [135]
EV71 virus	QD/GO	1 to 15 ng/mL	0.38 ng/mL	Ref. [136]
CVB3 virus	QD/GO	1 to 14 ng/mL	0.26 ng/mL	Ref. [136]

4.2 AuNPs as FRET acceptors

Gold nanoparticle (AuNP), a nano-scaled particle created from gold, is probably the most remarkable member among metal nanoparticles owing to its excellent properties, including surface plasmon resonance phenomena, good conductivity, easy surface modification, and high fluorescence quenching capability.[137-138] Generally, AuNPs are used as highly efficient long-range fluorescence acceptors in biological and medical applications due to its super quenching efficiency in a wide spectra range.[139-141] Unlike other dye molecules, the spherical AuNPs have no defined dipole moment, leading to possibility of energy transfer to AuNPs in any orientation of the donor relative to the surface of the AuNPs.[141] In this case, the energy transfer from fluorophore to spherical AuNPs is not an oscillating point dipoles, but a collective resonant oscillation caused by dipole-surface effects which possess (distance)-4 dependent energy transfer efficiency,[142] thereby leading to higher efficiency as compared to that ((distance)-6) of traditional FRET. The distance between donors to AuNPs was calculated to be as long as 70-100 nm,[142] which is almost ten times longer than conventional FRET. Additionally, the absorption spectra of AuNPs have large cross section near the plasmon resonance frequency range, which enhances their performance as energy acceptors. The high surface to volume ratio of AuNPs also contributes to the enhancement of FRET efficiency by providing a configuration of multiple-donor-single-acceptor. Furthermore, the ease of surface immobilization of oligonucleotide onto AuNPs, facilitate the development of AuNPs based FRET system in numerous applications.[143-144]

Tang et al. designed a QDs-ConA-β-CDs-AuNPs nanocomplex based on FRET strategy for glucose detection.[145] ConA-conjugated CdTe QDs was used as FRET donor, while β-CDs-AuNPs was employed as FRET acceptor. FRET occurred when the distance between donor and acceptor was shortened by the specific combination, forming the nanocomplex of QDs-ConA-β-CDs-AuNPs. Upon addition of glucose, β-CDs-AuNPs was replaced by glucose, resulting in the fluorescence recovery. By monitoring the signal change, a linear working curve of fluorescence intensity could be obtained as a function of glucose concentration of 0.10–50 μM. The detection limit of this assay for glucose detection was 50 nM.

For DNA analysis, Dubertret et al. initially fabricated a highly quenched molecular beacon labeled by AuNPs and organic fluorescent dyes for sensitive detection of target DNA.[146] After specific hybridization with complimentary DNA, the molecular beacon was opened which resulted in recovered fluorescence intensity. By monitoring the fluorescence signal change, the sensitivity of this molecular beacon was enhanced up to 100-fold as compared to typical molecular beacon. Dyadyusha et al. also investigated the quenching ability of AuNPs based on DNA hybridization, but they replaced the organic fluorescent dyes with QDs.[147] The emission of QDs was highly quenched by contact with AuNPs with energy transfer efficiency as high as 85%. Maxwell et al. developed a constrained conformation between AuNPs and fluorescent dyes linked by oligonucleotide molecules for detection of specific DNA sequence.[148] Initially the fluorescence of organic dyes was quenched by AuNPs at assembled state. Upon addition of target DNA, the fluorescence intensity was restored

due to the conformation change. The quenching efficiency of AuNPs nearly reached 100%.

AuNPs have been used as acceptor molecules in many FRET immunoassays. Kato et al. established a homogeneous AuNP/polyelectrolyte coated latex particle based FRET immunoassay for biotin molecule detection.[149] Initially, the fluorescence signal of fluorescein isothiocyanate labeled anti-biotin immunoglobulin (FITC-anti-biotin IgG) was quenched by AuNP/polyelectrolyte (AuNP/PE) coated latex particles. In the presence of injected biotin, the specific binding between biotinylated poly (allylamine hydrochloride) (B-PAH) layer and biotin would result in the release of FITC-biotin, leading to the recovery of fluorescence signals. A dynamic sensing range of 1-50 nmol was achieved. Oh et al. investigated the FRET effect between streptavidin coated QDs (donor) and biotinylated AuNPs (acceptor) and demonstrated that this sensing system could be used as bimolecular inhibition assay.[150] The fluorescence intensity of QDs was quenched by AuNPs due to the streptavidin-biotin interaction, which brought QD and AuNPs into close proximity and triggered FRET. For avidin detection, the specific binding between avidin and biotinylated AuNPs would break previous quenched QDs-AuNPs system, causing the change of fluorescence intensity. The LOD of this FRET assay for avidin detection was around 10 nM. Recently, Chen et al. developed an AuNP based FRET competitive immunoassay for human immunoglobulinM (IgM) detection.[151] The combination between FITC and AuNPs caused the fluorescence quenching of FITC. Upon the binding with target antigen, FITC labeled antigen detached from AuNPs due

to the competitive immuno-reaction, leading to the recovery of fluorescence signal. This competitive immunoassay had a detection limit of 42 pM for IgM detection.

AuNPs based FRET immunoassays have also been used for human disease biomarker detection. Mayilo et al. reported a homogeneous sandwich immunoassay based on fluorescence dyes and AuNPs for the detection of the protein cardiac troponin T (cTnT).[141] Cy3 labeled M7 antibody was served as fluorescent donor, while anti-cTnT M11.7 antibody conjugated AuNPs were used as fluorescence quenchers. As cTnT could specifically bind to two different antibodies, the sandwich formation of AuNP- M11.7-cTnT- M7-Cy3 would shorten the distance between AuNPs and Cy3, thus leading to FRET effect. This AuNPs based FRET biosensor could achieve a detection limit as low as 0.02 nM for cTnT detecion. Park et al. developed an AuNP based fluorescence quenching system via metal coordination for matrix metalloproteinase-7 (MMP-7) detection.[152] Carboxy AuNPs linked with the hexahistidine regions of dye-tethered peptides in the presence of Ni(II) ions, leading to the fluorescence quenching of dyes. With the addition of MMP-7, fluorescence signal was recovered by the cleavage of the linking peptide. The detection limit of this AuNP FRET assay was around 10 ng/mL.

A summary that lists the applications of AuNP FRET assays and their sensing parameters is provided in Table 7.

Table 7 Summary of AuNP FRET assays and their sensing parameters

Biological targets	Donor/Acceptor	Detection range	Limit of detection	References
Glucose	QD/AuNP	0.10–50 μM	50 nM	Ref. [145]
DNA hybridization	Fluorophore/AuNP	67 pM to 13 μM	67 pM	Ref. [146]
IgG	Fluorophore/AuNP	1 to 50 nmol	1 nmol	Ref. [149]
Avidin	QD/AuNP	10 nM to 2 μM	10 nM	Ref. [150]
IgM	Fluorophore/AuNP	0.35 to 5 nM	42 pM	Ref. [151]
cTnT	Fluorophore/AuNP	0.02 to 0.15 nM	0.02 nM	Ref. [141]
MMP-7	Fluorophore/AuNP	10 to 1,000 ng/mL	10 ng/mL	Ref. [152]

5. Conclusion and future perspectives

In the past years, great progress has been seen for nanoparticle based FRET systems in biosensing field with higher efficiency and better performance compared with traditional FRET systems based on organic fluorophores. In this review, we mainly focuses on the recent development of utilization of nanoparticles as donors including semiconductor quantum dots (QDs), graphene quantum dots (GQDs) and rare-earth doped upconversion nanoparticles (UCNPs), and nanoparticles as acceptors including gold nanoparticles (AuNPs) and graphene oxide (GO) for various bioanalysis applications. Compared with traditional organic fluorophores, nanoparticle FRET donors have stronger fluorescence signal, longer fluorescence life time and higher stability; nanoparticle FRET acceptors have advantages including super quenching efficiency and long quenching distance. For the real applications of

nanoparticle FRET assay, the cost consideration is critical. For example, the significant cost consideration of AuNP is a fundamental limitation for its wide applications. It is important to look for new fabrication methods or new nanoparticles to decrease the cost. Mass production methods have been explored for QDs, and UCNPs, which could significantly decrease the cost. Especially, graphene based materials not only have a very low cost due to the carbon based raw materials and the established large scale production methods, but also can be used as both donors such as 0D grapheme material-GQDs, and acceptors such as 2D grapheme material-GO sheets. These advantages make graphene based materials promising candidates for low-cost nanoparticle FRET assays. The focus of future nanoparticle FRET assays for bioanalysis should be on designing biocompatible FRET pairs with high FRET efficiency and sensitivity, good specificity, high stability, and low cost for both *in vitro* and *in vivo* applications.

References

1 R. M. Clegg, *Curr. Opin. Biotechnol.*, 1995, **6**, 103-110.
2 P. R. Selvin, *Nat. Struct. Biol.*, 2000, **7**, 730-734.
3 T. Forster, *Naturwissenschaften*, 1946, **33**, 166-175.
4 T. Ha, T. Enderle, D. Ogletree, D. Chemla, P. Selvin and S. Weiss, *Proc Natl Acad Sci.*, 1996, **93**, 6264-6268.
5 R. Heim and R. Y. Tsien, *Curr. Biol.*, 1996, **6**, 178-182.
6 J. Franck, *Z. Phys. A-hadron. Nucl.*, 1922, **9**, 259-266.
7 G. Cario and J. Franck, *Z. Phys. A-hadron. Nucl.*, 1922, **11**, 161-166.
8 J. Perrin, CR Hebd. *Seances Acad. Sci*, 1927, 184, 1097-1100.
9 F. Perrin, Ann. *Phys.(Paris)*, 1932, **12**, 283-314.
10 H. Kallmann, and F. London,*Z. Phys. Chem.*, 1928, **B2**, 207-243.
11 F. Perrin. Ann. *Phys. (Paris)*, 1929, **12**, 169-275
12 T. Förster, *Ann phys-Berlin*, 1948, **437**, 55-75.
13 H. Dong, W. Gao, F. Yan, H. Ji and H. Ju, *Anal. Chem.*, 2010, **82**, 5511-5517.

14 E. Oh, M.Y. Hong, D. Lee, S.H. Nam, H. C. Yoon and H.S. Kim, *J. Am. Chem. Soc.*, 2005, **127**, 3270-3271.

15 R. Gill, I. Willner, I. Shweky and U. Banin, *J. Phys. Chem. B*, 2005, **109**, 23715-23719.

16 R. B. Sekar and A. Periasamy, *J. Cell Bio.*, 2003, **160**, 629-633.

17 V. Sourjik and H. C. Berg, *Proc Natl Acad Sci.*, 2002, **99**, 12669-12674.

18 V. V. Didenko, *Biotechniques*, 2001, **31**, 1106.

19 A. N. Glazer and R. A. Mathies, *Curr. Opin. Biotechnol.*, 1997, **8**, 94-102.

20 J. Ju, I. Kheterpal, J. R. Scherer, C. Ruan, C. W. Fuller, A. N. Glazer and R. A. Mathies, *Anal. Biochem.*, 1995, **231**, 131-140.

21 O. Shimomura, F. H. Johnson and Y. Saiga, *J. Cell. Comp. Physiol.*, 1962, **59**, 223-239.

22 M. Chalfie, *Proc Natl Acad Sci.*, 2009, **106**, 10073-10080.

23 R. Y. Tsien, *Annu. Rev. Biochem.*, 1998, **67**, 509-544.

24 G. N. Phillips, *Curr. Opin. Struct. Biol.*, 1997, **7**, 821-827.

25 R. Y. Tsien, *FEBS Lett.*, 2005, **579**, 927-932.

26 G. H. Patterson, D. W. Piston and B. G. Barisas, *Anal. Biochem.*, 2000, **284**, 438-440.

27 M. Fehr, W. B. Frommer and S. Lalonde, *Proc Natl Acad Sci.*, 2002, **99**, 9846-9851.

28 H. Grecco, K. Lidke, R. Heintzmann, D. Lidke, C. Spagnuolo, O. Martinez, E. Jares‐Erijman and T. Jovin, *Microsc. Res. Tech.*, 2004, **65**, 169-179.

29 K. E. Sapsford, L. Berti and I. L. Medintz, *Angew. Chem. Int. Ed.*, 2006, **45**, 4562-4589.

30 N. McGrath and M. Barroso, *J. Biomed. Opt.*, 2008, **13**, 031210-031210-031219.

31 I. L. Medintz and H. Mattoussi, *Phys. Chem. Chem. Phys.*, 2009, **11**, 17-45.

32 W. K. Leutwyler, S. L. Bürgi and H. Burgl, *Science*, 1996, **271**, 933-937.

33 M. Nirmal and L. Brus, *Acc. Chem. Res.*, 1999, **32**, 407-414.

34 Y. Zhang and T.H. Wang, *Theranostics*, 2012, **2**, 631.

35 W. R. Algar and U. J. Krull, *Anal. Bioanal. Chem.*, 2008, **391**, 1609-1618.

36 U. Resch-Genger, M. Grabolle, S. Cavaliere-Jaricot, R. Nitschke and T. Nann, *Nat. Methods*, 2008, **5**, 763-775.

37 M. A. Hines and P. Guyot-Sionnest, *J. Phys. Chem.*, 1996, **100**, 468-471.

38 L. Mattsson, K.D. Wegner, N. Hildebrandt and T. Soukka,, *RSC Advances*, 2015, **5,** 13270-13277.

39 H. Xu, X.M. Huang, W.J. Zhang, G.J. Chen, W.H. Zhu, X.H. Zhong, *Chemphyschem*, 2010, **11,** 3167-3171**.**

40 C. Y. Zhang, H. C. Yeh, M. T. Kuroki and T. H. Wang, *Nat. Mater*, 2005, **4**, 826-831.

41 W. R. Algar and U. J. Krull, *Anal. chem.*, 2009, **81**, 4113-4120.

42 W. R. Algar and U. J. Krull, *Langmuir*, 2009, **26**, 6041-6047.

43 W. R. Algar and U. J. Krull, *Langmuir*, 2008, **25**, 633-638.

44 J. H. Kim, D. Morikis and M. Ozkan, *Sensor. Actuat. B: Chem.*, 2004, **102**, 315-319.

45 Q. Wei, Q, M. Lee, X. Yu, E.K. Lee, G.H. Seong, J. Choo and Y.W. Cho, *Anal Biochem.*, 2006, **358**, 31-37.

46 C.W. Chi, Y.H. Lao, Y.S. Li and L.C. Chen, *Biosens Bioelectron.* 2011, **26**, 3346-52,

47 M.K. Wagner, F. Li, J. Li, X.F. Li and X.C. Le, *Anal Bioanal Chem.* 2010, **397,** 3213-24.

48 M. Suzuki, Y. Husimi, H. Komatsu, K. Suzuki and K.T. Douglas. *J Am Chem Soc.,* 2008*,* **130,** 5720-25.

49 I. Yildiz, X. Gao, T.K. Harris and F.M. Raymo. 2007, *J Biomed Biotechnol.,* 2007, 18081.

50 A.M. Dennis, W.J. Rhee, D. Sotto, S.N. Dublin and G. Bao, *ACS Nano,* 2012, **6**, 2917-24.

51 H.Y. Liu, G.X. Liang, E.S. Abdel-Halim and J.J. Zhu, *Analytical Methods,* 2011,**3,** 1797-1801.

52 A.K.H. Cheng, H.P. Su, A. Wang and H.Z. Yu, *Anal Chem.,* 2009, **81**, 6130-6139.

53 K. Boeneman, B.C. Mei, A.M. Dennis, G. Bao, J.R. Deschamps, H. Mattoussi and I.L. Medintz, *J Am Chem Soc.,* 2009, **131,** 3828-29.

54 Y. Choi, Y. Cho, M. Kim, R. Grailhe and R. Song, *Anal. Chem., 2012,* **84**, 8595-8601.

55 A. ukhanova and I. Nabiev, *Crit Rev Oncol Hematol.*, *2008*, **68**, 39–59.

56 K. Boeneman, J. R. Deschamps, S. B. White, D. E. Prasuhn, J. B. Canosa, P. E. Dawson, M. H. Stewart, K. Susumu, E. R. Goldman and M. Ancona, *Acs Nano*, 2010, **4**, 7253-7266.

57 W. Wu, J. Shen, P. Banerjee and S. Zhou, *Biomaterials*, 2010, **31**, 7555-7566.

58 J. Gao, K. Chen, Z. Miao, G. Ren, X. Chen, S. S. Gambhir and Z. Cheng, *Biomaterials*, 2011, **32**, 2141-2148.

59 J. M. Li, M. X. Zhao, H. Su, Y. Y. Wang, C. P. Tan, L.. N. Ji and Z. W. Mao, *Biomaterials*, 2011, **32**, 7978-7987.

60 A. K. Geim and K. S. Novoselov, *Nature Mater.*, 2007, **6**, 183-191.

61 K. S. Novoselov, D. Jiang, F. Schedin, T. J. Booth, V. V. Khotkevich, S. V. Morozov, and A. K. Geim. *Proc Natl Acad Sci U S A*, 2005, **102**, 10451-3.

62 L. S. Li and X. J. Yan, *Phys. Chem. Lett.*, 2010, **1**, 2572-2576.

63 D. Pan, J. Zhang, Z. Li, and M. Wu, *Adv. Mater.*, 2010. **22**, 734-738.

64 Y. Li, Y. Hu, Y. Zhao, G. Shi, L. Deng, Y. Hou, and L. Qu, *Adv. Mater.*, 2011, **23**, 776-780.

65 M. Zhang, L. Bai, W. Shang, W. Xie, H. Ma, Y. Fu, D. Fang, H. Sun, L. Fan and M. Han, *J. Mater. Chem.*, 2012, **22**, 7461-7467.

66 C. Hu, Y. Liu, Y. Yang, J. Cui, Z. Huang, Y. Wang, L. Yang, H. Wang, Y. Xiao and J. Rong, *J. Mater. Chem. B*, 2013, **1**, 39-42.

67 S. Kim, S. W. Hwang, M. K. Kim, D. Y. Shin, D. H. Shin, C. O. Kim, S. B. Yang, J. H. Park, E. Hwang and S. H. Choi, *ACS nano*, 2012, **6**, 8203-8208.

68 H. Tetsuka, R. Asahi, A. Nagoya, K. Okamoto, I. Tajima, R. Ohta and A. Okamoto, *Adv. Mater.*, 2012, **24**, 5333-5338.

69   F. Liu, M. H. Jang, H. D. Ha, J. H. Kim, Y. H. Cho and T. S. Seo, *Adv. Mater.*, 2013, **25**, 3657-3662.

70   J. Shen, Y. Zhu, C. Chen, X. Yang and C. Li, *Chem. Commun.*, 2011, **47**, 2580-2582.

71   F. Yang, M. Zhao, B. Zheng, D. Xiao, L. Wu and Y. Guo, *J. Mater. Chem.*, 2012, **22**, 25471-25479.

72   S. Zhu, J. Zhang, S. Tang, C. Qiao, L. Wang, H. Wang, X. Liu, B. Li, Y. Li and W. Yu, *Adv. Funct. Mater.*, 2012, **22**, 4732-4740.

73   S. Zhuo, M. Shao and S. T. Lee, *ACS nano*, 2012, **6**, 1059-1064.

74   S. Zhu, J. Zhang, C. Qiao, S. Tang, Y. Li, W. Yuan, B. Li, L. Tian, F. Liu and R. Hu, *Chem. Commun.*, 2011, **47**, 6858-6860.

75   X. Yan, X. Cui, B. Li and L. S. Li, *Nano Lett.*, 2010, **10**, 1869-1873.

76   X. Zhou, Y. Zhang, C. Wang, X. Wu, Y. Yang, B. Zheng, H. Wu, S. Guo and J. Zhang, *Acs Nano*, 2012, **6**, 6592-6599.

77   S. S. Kim, J. Y. Choi, K. Kim and B. H. Sohn, *Nanotechnology*, 2012, **23**, 125301.

78   L. Fan, Y. Hu, X. Wang, L. Zhang, F. Li, D. Han, Z. Li, Q. Zhang, Z. Wang and L. Niu, *Talanta*, 2012, **101**, 192-197.

79   L. Zhang, Y. Xing, N. He, Y. Zhang, Z. Lu, J. Zhang and Z. Zhang, *J. Nanosci. Nanotechnol.*, 2012, **12**, 2924-2928.

80   J. Peng, W. Gao, B. K. Gupta, Z. Liu, R. Romero-Aburto, L. Ge, L. Song, L. B. Alemany, X. Zhan and G. Gao, *Nano Lett.*, 2012, **12**, 844-849.

81   Z. Liu, J. T. Robinson, X. Sun and H. Dai, *J. Am. Chem. Soc.*, 2008, **130**, 10876-10877.

82   J. Shi, C. Chan, Y. Pang, W.W. Ye, F. Tian, J. Lyu, Y. Zhang and M. Yang, *Biosens Bioelectron.*, 2015, **67**, 595-600.

83   Z.S. Qian, X.Y. Shan, L.J. Chai, J.J. Ma, J.R. Chen and H. Feng, *Biosens Bioelectron.* 2014, **60**, 64-70.

84   Z.S. Qian, X.Y. Shan, L.J. Chai, J.J. Ma, J.R. Chen and H. Feng, *Nanoscale*, 2014, **6**, 5671-74.

85   H. Zhao, Y. Chang, M. Liu, S. Gao, H. Yu and X. Quan, *Chem. Commun.*, 2013, **49**, 234-236.

86   L. Fan, Y. Hu, X. Wang, L. Zhang, F. Li, D. Han, Z. Li, Q. Zhang, Z. Wang and L. Niu, *Talanta.* 2012, **101**, 192-7.

87   M. Haase and H. Schäfer, *Angew. Chem. Int. Edit.*, 2011, 50, 5808-5829.

88   F. Auzel, *Chem. Rev.*, 2004, **104**, 139-174.

89   Z. Li and Y. Zhang, *Angewandte Chemie.*, **2006**, *118*, 7896-7899.

90   K. W. Krämer, D. Biner, G. Frei, H. U. Güdel, M. P. Hehlen and S. R. Lüthi, *Chem. Mater.*, **2004**, *16*, 1244-1251.

91   C. Zhang, P. Ma, C. Li, G. Li, S. Huang, D. Yang, M. Shang, X. Kang and Lin, *J. Mater. Chem.*, **2011**, *21*, 717-723.

92   S. Zeng, M. Tsang, C. Chan, K. Wong, B. Fei and J. Hao, *Nanoscale.*, **2012**, *4*, 5118-5124.

93 G.Y. Chen, Y. Liu, Z.G. Zhang, B. Aghahadi, G. Somesfalean, Q. Sun and F.P. Wang, *Chem. Phys. Lett.,* **2007**, *448*, 127-131.

94 J.Y. Liao, Z.W. Yang, H.J. Wu, D. Yan, J.B. Qiu, Z.G. Song, Y. Yang, D.C. Zhou and Z.Y. Yin, *J. Mater. Chem. C.*, **2013, 1,** 6541-6546.

95 W. Gao, R.B. Wang, Q.Y. Han, J. Dong, L.X. Yan and H.R. Zheng, *J. Phys. Chem. C.,* **2015,** *119,* 2349–2355.

96 D. Ma, D. Yang, J. Jiang, P. Cai and S. Huang, *Cryst Eng Comm,* 2010, **12**, 1650-1658.

97 P. Zhang, S. Rogelj, K. Nguyen and D. Wheeler, *J. Am. Chem. Soc.*, 2006, **128**, 12410-12411.

98 Z. Chen, H. Chen, H. Hu, M. Yu, F. Li, Q. Zhang, Z. Zhou, T. Yi and C. Huang, *J. Am. Chem. Soc.*, 2008, **130**, 3023-3029.

99 S.H. Hwang, S.G. Im, H. Sung, S.S. Hah, V.T. Cong, D.H. Lee, S.J. Son and H.B. Oh, *Biosens Bioelectron,* **2014,** *53,* 112-116.

100 D. Tu, L. Liu, Q. Ju, Y. Liu, H. Zhu, R. Li and X. Chen, *Angew. Chem. Int. Edit.,* 2011, **50**, 6306-6310.

101 Q. Ju, D. Tu, Y. Liu, R. Li, H. Zhu, J. Chen, Z. Chen, M. Huang and X. Chen, *J. Am. Chem. Soc.*, 2011, **134**, 1323-1330.

102 S. Wu, N. Duan, X. Ma, Y. Xia, H. Wang, Z. Wang and Q. Zhang, *Anal. Chem.*, 2012, **84**, 6263-6270.

103 C. Liu, Z. Wang, H. Jia and Z. Li, *Chem. Commun.*, 2011, **47**, 4661-4663.

104 C. Zhang, Y. Yuan, S. Zhang, Y. Wang and Z. Liu, *Angew. Chem. Int. Ed.*, 2011, **50**, 6851-6854.

105 P. Alonso-Cristobal, P. Vilela, A. El-Sagheer, E. Lopez-Cabarcos, T. Brown, O.L. Muskens, J. Rubio-Retama and A.G. Kanaras, *ACS Appl. Mater. Interfaces,* 2015, **7**, 12422−12429.

106 Y.H. Wang, P. Shen, C.Y. Li, Y.Y. Wang and Z.H. Liu, *Ana. Chem.,* 2012, **84***,* 1466-1473.

107 W. W. Ye, M. K. Tsang, X. Liu, M. Yang and J. Hao, *Small*, 2014, **10**, 2390-2397.

108 L. Wang, R. Yan, Z. Huo, L. Wang, J. Zeng, J. Bao, X. Wang, Q. Peng and Y. Li, *Angew. Chem. Int. Ed.*, 2005, **44**, 6054-6057.

109 M. Wang, W. Hou, C. C. Mi, W. X. Wang, Z. R. Xu, H. H. Teng, C. B. Mao and S. K. Xu, *Anal. Chem.*, 2009, **81**, 8783-8789.

110 Q. Long, H. Li, Y. Zhang and S. Yao, *Biosens Bioelectron, 2015,* **68**, 168–174.

111 Y. P. Kim, Y. H. Oh, E. Oh, S. Ko, M. K. Han and H. S. Kim, *Anal. Chem.*, 2008, **80**, 4634-4641.

112 M.O. Noor, A. Shahmuradyan and U.J. Krull, *Anal. Chem.*, *2013,* **85,** 1860-1867.

113 J.H. Jung, D.S. Cheon, F. Liu, K.B. Lee, T.S. Seo, *Angew. Chem. Int. Ed*., 2010, **49,** 5708-5711.

114 Y. Shi, J.Z. Wu, Y.J. Sun, Y. Zhang, Z.W. Wen, H.C. Dai, H.D. Wang, Z. Li, *Biosens Bioelectron*, 2012, **38**, 31-36.

115 S. William, J. Hummers and R. Offeman, *J. Am. Chem. Soc.*, 1958, **80**, 1339.

116 D. R. Dreyer, S. Park, C. W. Bielawski and R. S. Ruoff, *Chem. Soc. Rev.* 2010, **39**, 228-240.

117 J. Kim, L. J. Cote, F. Kim and J. Huang, *J. Am. Chem. Soc.*, 2009, **132**, 260-267.

118 M. Wu, R. Kempaiah, P.-J. J. Huang, V. Maheshwari and J. Liu, *Langmuir*, 2011, **27**, 2731-2738.

119 S. Li, A. N. Aphale, I. G. Macwan, P. K. Patra, W. G. Gonzalez, J. Miksovska and R. M. Leblanc, *ACS Appl. Mater. Interfaces*, 2012, **4**, 7069-7075.

120 N. P. Mahajan, K. Linder, G. Berry, G. W. Gordon, R. Heim and B. Herman, *Nat. Biotechnol.*, 1998, **16**, 547-552.

121   H. Dong, W. Gao, F. Yan, H. Ji and H. Ju, *Anal. Chem.*, 2010, **82**, 5511-5517.

122   C. Liu, Z. Wang, H. Jia and Z. Li, *Chem. Commun.*, 2011, **47**, 4661-4663.

123   R. Swathi and K. Sebastian, *J chem. Phys.*, 2009, **130**, 086101.

124   R. Swathi and K. Sebastian, *J. Chem. Phys.*, 2008, **129**, 054703.

125   P.J. J. Huang and J. Liu, *Anal. Chem.*, 2012, **84**, 4192-4198.

126   S. Stankovich, D. A. Dikin, G. H. Dommett, K. M. Kohlhaas, E. J. Zimney, E. A. Stach, R. D. Piner, S. T. Nguyen and R. S. Ruoff, *Nature*, 2006, **442**, 282-286.

127   J. Kim, L. J. Cote, F. Kim, W. Yuan, K. R. Shull and J. Huang, *J. Am. Chem. Soc.*, 2010, **132**, 8180-8186.

128   Y. Piao, F. Liu and T. S. Seo, *Chem. Commun.*, 2011, **47**, 12149-12151.

129   S. He, B. Song, D. Li, C. Zhu, W. Qi, Y. Wen, L. Wang, S. Song, H. Fang and C. Fan, *Adv. Funct. Mater.*, 2010, **20**, 453-459.

130 C. H. Lu, J. Li, J. J. Liu, H. H. Yang, X. Chen and G. N. Chen, *Chem-Eur. J.*, 2010, **16**, 4889-4894.

131 J. Shi, J. Guo, G. Bai, C. Chan, X. Liu, W. Ye, J. Hao, S. Chen and M. Yang, *Biosensors Bioelectron.*, 2015, **65**, 238-244.

132 D. Feng, Y. Zhang, T. Feng, W. Shi, X. Li and H. Ma, *Chem. Commun.*, 2011, **47**, 10680-10682.

133 E.Q. Song, D. Cheng, Y. Song, M.D. Jiang, J.F. Yu and Y.Y. Wang, *Biosens Bioelectron.,2013,* **47***, 445-450.

134 Z. Wang, P. Huang, A. Bhirde, A. Jin, Y. Ma, G. Niu, N. Neamati and X. Chen, *Chem. Commun.*, 2012, **48**, 9768-9770.

135 S.E. Wang and S.H. Si, *Applied Spectroscopy*, 2013, **67**, 1270-1274.

136 L. Chen, X. Zhang, G. Zhou, X. Xiang, X. Ji, Z. Zheng, Z. He and H. Wang, *Anal. Chem.*, 2012, **84**, 3200-3207.

137 S. Eustis and M. A. El-Sayed, *Chem. Soc. Rev.*, 2006, **35**, 209-217.

138 M. C. Daniel and D. Astruc, *Chem. Rev.*, 2004, **104**, 293-346.

139 E. Oh, M. Y. Hong, D. Lee, S. H. Nam, H. C. Yoon and H. S. Kim, J. Am. Chem. Soc., 2005, 127, 3270-3271.

140 P. C. Ray, G. K. Darbha, A. Ray, W. Hardy and J. Walker, *Nanotechnology*, 2007, **18**, 375504.

141 S. Mayilo, M. A. Kloster, M. Wunderlich, A. Lutich, T. A. Klar, A. Nichtl, K. Kurzinger, F. D. Stefani and J. Feldmann, *Nano Lett.*, 2009, **9**, 4558-4563.

142 J. Gersten and A. Nitzan, *J. Chem. Phys.*, 1981, **75**, 1139-1152.

143 C. A. Mirkin, R. L. Letsinger, R. C. Mucic and J. J. Storhoff, *Nature*, 1996, 607-609.

144 P. C. Ray, G. K. Darbha, A. Ray, J. Walker and W. Hardy, *Plasmonics*, 2007, **2**, 173-183.

145 B. Tang, L. Cao, K. Xu, L. Zhuo, J. Ge, Q. Li and L. Yu, *Chem-Eur. J.,* 2008, **14**, 3637-3644.

146 B. Dubertret, M. Calame and A. J. Libchaber, *Nat. Biotechnol.*, 2001, **19**, 365-370.

147 L. Dyadyusha, H. Yin, S. Jaiswal, T. Brown, J. Baumberg, F. Booy and T. Melvin, *Chem. Commun.*, 2005, 3201-3203.

148 D. J. Maxwell, J. R. Taylor and S. Nie, *J. Am. Chem. Soc.*, 2002, **124**, 9606-9612.

149 N. Kato and F. Caruso, *J. Phys. Chem. B*, 2005, **109**, 19604-19612.

150 E. Oh, M. Y. Hong, D. Lee, S. H. Nam, H. C. Yoon and H. S. Kim, *J. Am. Chem. Soc.*, 2005, **127**, 3270-3271.

151 J. Chen, Y. Huang, S.L. Zhao, X. Lu and J.N. Tian, *Analyst*, 2012, **137**, 5885-5890.

152 S.Y. Park, S.M. Lee, G.B. Kim and Y.P. Kim, *Gold Bull*, 2012, **45**, 213–219